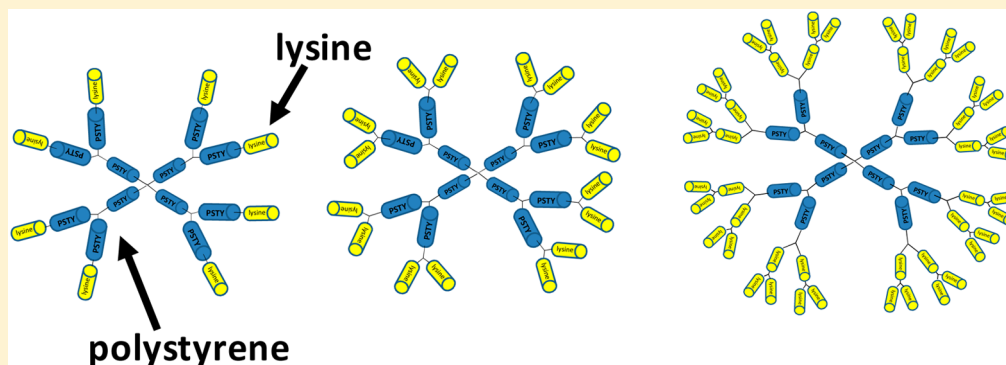


One-Pot Orthogonal Copper-Catalyzed Synthesis and Self-Assembly of L-Lysine-Decorated Polymeric Dendrimers

Derong Lu, Md. D. Hossain, Zhongfan Jia, and Michael J. Monteiro*

Australian Institute for Bioengineering and Nanotechnology, The University of Queensland, Brisbane QLD 4072, Australia

S Supporting Information



ABSTRACT: Synthetic peptides, including cyclic peptides and peptidomimetics, provide stability, protection, and long circulation times compared to free-circulating peptides. Dendritic structures with amino acids or peptides attached to the peripheral layer represent one form of peptidomimetics (i.e., a hybrid peptide/dendrimer construct) that has found use in biological applications. Constructing such dendritic structures from linear polymeric building blocks provides a further advantage of generating a highly ordered and defined structure in the nanoparticle size range. However, the rapid synthesis of such well-defined structures is still a challenge. In this work, we demonstrate that through modulating the copper activity concomitantly of the nitroxide radical coupling (NRC) and the azide–alkyne cycloaddition (CuAAC) reactions, polymeric dendrimers decorated with L-lysine on the periphery could be made rapidly in one pot at 25 °C. Three polymeric dendrimers were constructed with high purity (>94%) and with varying L-lysine density coated on the peripheral generation layer. The self-assembly of these dendrimers in water gave similar sizes to that found in organic solvents, suggesting that the aggregation number of dendritic structures in water was very low and possibly consisting of unimolecular micelles. The findings support the conclusion that the self-assembly of a dendritic architecture in water produces nanoparticles with predictable and well-controlled sizes. This synthetic methodology and the self-assembly properties represent an important step toward synthesizing peptide-decorated dendrimers targeted toward therapeutic applications.

INTRODUCTION

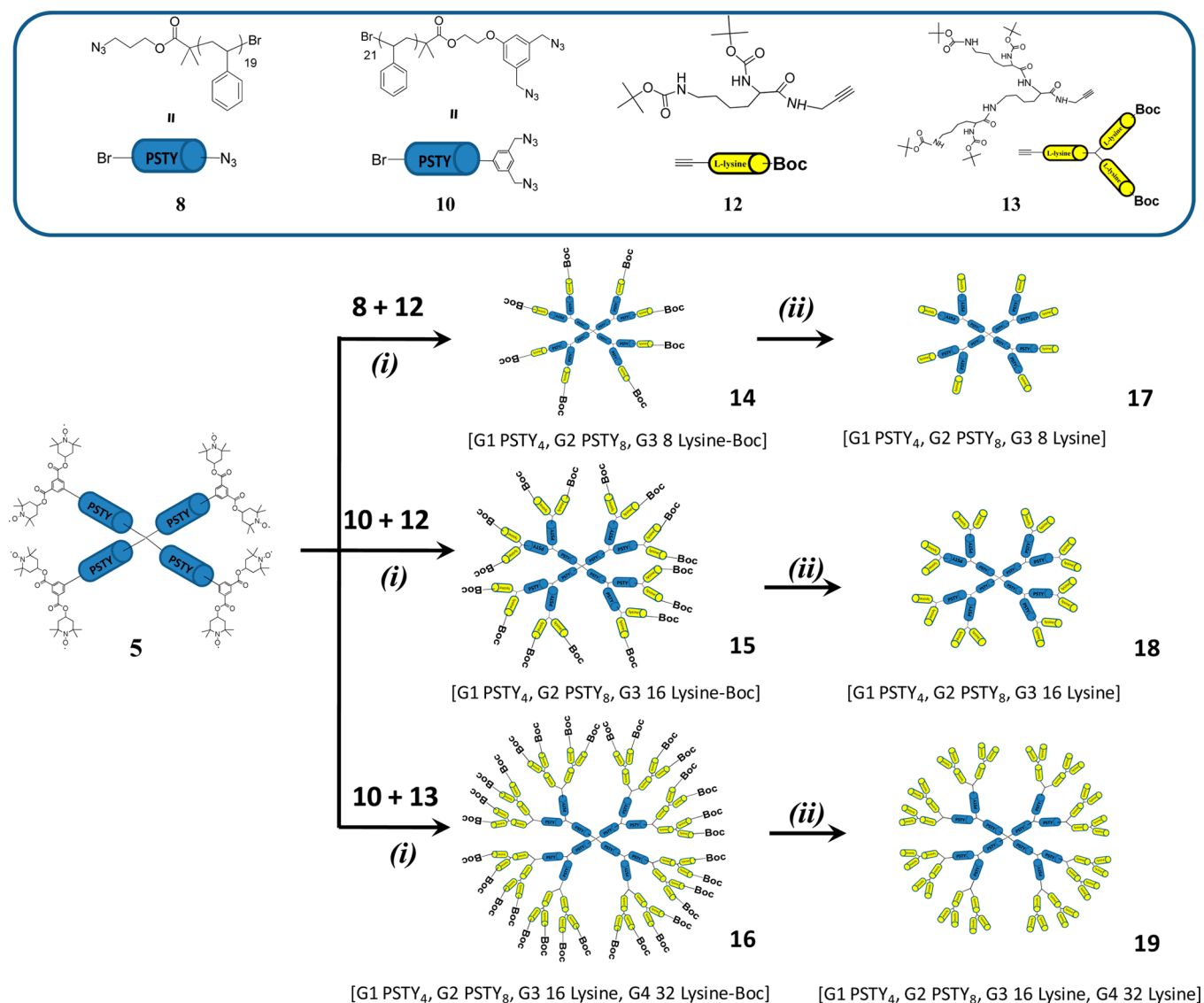
Recently, there has been a rapid increase in the number of synthetic peptides with therapeutic efficacy covering a diverse range of bioapplications.¹ The synthesis of cyclic peptides and peptidomimetics helped to overcome many of the drawbacks limiting the use of peptides as therapeutics in the past. These drawbacks included low stability in plasma, rapid degradation by proteases, and rapid clearance from circulation.² Synthetic peptides in the form of dendrimers (i.e., peptidomimetics) were found to be much more stable when incubated with human plasma and serum.³ Dendrimers consisting of a fourth-generation poly(L-lysine) with multivalent ligands on the peripheral generational layer are in clinical trials as an antiviral topical ointment.^{4,5} Although dendrimers built from small molecules in each generation (with sizes <15 nm) have been widely researched for many biological applications,^{6,7} dendrimers synthesized from polymeric building blocks^{8–15} (denoted here as polymeric dendrimers) have extended the

applications to where larger sizes (>15 nm) were required, including a self-adjuncting vaccine¹⁶ and a cancer vaccine.¹⁷ Polymeric dendrimers combine the attributes of the highly branched and symmetrical dendrimer structure, consisting of well-defined functionality within the generational layers and periphery, with the advantages of size and shape associated with nanoparticles.^{13,18}

Considerable work has been carried out to produce a wide range of polymeric dendrimers either through divergent or convergent methods.^{8,9,11,14,19–21} One of the first strategies to combine “living” radical polymerization (LRP) and a chain-end coupling process was denoted as TERMINI (terminator multifunctional initiator), in which polymers were divergently grown via LRP, terminated with a difunctional molecule that

Received: January 28, 2015

Revised: February 24, 2015

Scheme 1. Synthetic Route for Lysine Decorated Polymeric Third- and Fourth-Generational Layered Dendrimers^a

^a(i) One-pot, parallel CuAAC and NRC reaction. Polymer reactants with CuBr/PMDETA in a mixture of toluene/DMSO (50:50) for 30 min at 25 °C. (ii) Deprotection of Boc groups with TFA.

after deprotection acted as an initiator for further polymer growth—a process repeated until the desired generation was achieved.⁸ Other strategies included the divergent coupling of already synthesized linear polymers.¹¹ More recently, with the combination of LRP and “click” reactions, polymers were synthesized with precise control over their architecture, including stars,^{12,22} dendrimers,^{12,14,23–25} hyperbranched polymers,^{26–28} multiblock polymers,²⁹ and bioconjugates.^{30,31} There are now many examples of using “click” reactions to couple linear polymers together; these include the copper(I)-catalyzed azide–alkyne cycloaddition (CuAAC) reaction, strain-promoted azide–alkyne coupling (SPAAC),³² Diels–Alder,³³ and thiol–ene reactions.^{34–37}

Most dendrimers made from linear polymer building blocks are synthesized divergently in a sequential and iterative manner. This synthetic process requires multiple reaction steps, including protection and deprotection of terminal end-groups, and time-consuming purification before growth of the next generational layer. The use of orthogonal “click” coupling

reactions avoids many of these issues and increases the coupling efficiency with fewer reaction steps,^{37–39} but in many cases a change in experimental conditions are required for the next “click” reaction.

Here, we elaborate on a new process⁴⁰ of using two orthogonal “click”-type reactions (i.e., nitroxide radical coupling (NRC) and CuAAC) modulated by a copper catalyst to produce third- or fourth-generation layered polymer dendrimers that are densely coated with L-lysine groups in one pot at 25 °C (Scheme 1). This represents an advance on the previous techniques which relied on changing experimental conditions and purification at each generation step. By controlling the experimental conditions through selection of solvent and ligand, the synthesis of polymeric dendrimers in one pot could proceed via a divergent, convergent, or parallel process. The relative rates of the CuAAC and NRC reactions could be controlled to be comparable or with one significantly faster than the other. Utilizing the tool kit of building blocks shown in Scheme 1, the lysine peripheral density could be well

controlled. The purity of the foundational building block, **5**, is critical to the success of the polymer dendrimer synthesis. In general, the synthesis of 4-arm stars produces higher order star architectures through star–star radical coupling.⁴¹ Limiting the amount of star–star coupling allowed high-purity 4-arm star polymer to be produced, enabling the high peripheral density of L-lysine on the dendrimer. This method of producing well-defined polymeric dendrimers with densely decorated amino acids (or amino acid dendrons) on the periphery represents an important step toward synthetic peptides designed as therapeutics. To further validate the potential use for these dendrimers as peptidomimetic nanoparticles, the self-assembly of these structures in water was compared to that in organic solvent.

METHODS SECTION

Materials. Inhibitor was removed from styrene (STY: Aldrich, >99%) before use by passing through a basic alumina column. The following chemicals were used as received: alumina, activated basic (Aldrich, Brockmann I, standard grade, ~150 mesh, 58 Å), magnesium sulfate (MgSO₄: anhydrous, Scharlau, extra pure), sodium chloride (NaCl: Univar, 99.9%), sodium iodide (NaI: Aldrich, 99.5%), sodium azide (NaN₃: Aldrich, 99.5%), 1,1,1-triisopropylsilyl chloride (TIPS-Cl: Aldrich, 99%), tetrabutylammonium fluoride (TBAF: Aldrich, 1.0 M in THF), ethylmagnesium bromide solution (Aldrich, 3.0 M in diethyl ether), triethylamine (TEA: Fluka, 98%), TLC plates (silica gel 60 F254), silica gel 60 (230–400 mesh ATM (SDS)), potassium carbonate (K₂CO₃, AnalaR, 99.9%), 2-bromoisoobutyl bromide (BIB, Aldrich, 98%), lithium aluminum hydride (LiAlH₄, Aldrich, 98%), diphenylphosphoryl azide (DPPA, Aldrich, 97%), 1,8-diazabicyclo[5.4.0]undec-7-ene (DBU, Aldrich, 98%), tetrabutylammonium fluoride hydrate (TBAF, Aldrich, 1.0 M in THF), 18-crown-6 ether (18-C-6, Aldrich, 99%), 2-bromoethanol (Aldrich, 98%), imidazole (Aldrich, 99%) *N,N'*-dicyclohexylcarbodiimide (DCC, Aldrich, 99%), and *N*-hydroxysuccinimide (NHS, Aldrich, 98%).

The following solvents were used as received: acetone (Chem-Supply, AR), chloroform (CHCl₃: Labscan, AR grade), dimethyl sulfoxide (DMSO: Labscan, AR grade), dichloromethane (DCM: Labscan, AR grade), diethyl ether (Merck, GR grade), ethyl acetate (EtOAc: ChemSupply, AR grade), methanol (MeOH: anhydrous, Lichrosolv, 99.9%, HPLC grade), *N,N*-dimethylformamide (DMF: Labscan, AR grade), *N,N*-dimethylacetamide (DMAc: Aldrich, HPLC grade), petroleum spirit (BR 40–60 °C, Univar, AR grade), tetrahydrofuran (THF: Lichrosolv, HPLC grade), and toluene (TOL, Univar, AR grade).

The following initiators, ligands, and metals for the various polymerizations are given below and used as received unless otherwise stated: *N,N,N',N',N''*-pentamethyldiethylenetriamine (PMDETA: Aldrich, 99%), copper(II) bromide (Cu(II)Br₂: Aldrich, 99%), copper(I) bromide, and Cu(II)Br₂/PMDETA complex were synthesized in our group.

Analytical Methodologies. Size Exclusion Chromatography (RI-SEC). All polymer samples were dried prior to analysis in a vacuum oven for 2 days at 25 °C. The dried polymer was dissolved in tetrahydrofuran (THF) to a concentration of 1 mg mL⁻¹ and then filtered through a 0.45 μm PTFE syringe filter. The molecular weight distribution of the polymers was determined through separation on a Waters 2695 separations module, fitted with a Waters 410 refractive index (RI) detector maintained at 35 °C, a Waters 996 photodiode array detector, and two Ultrastaygel linear columns (7.8 × 300 mm) arranged in series. These columns were maintained at 40 °C for all analyses and are capable of separating polymers in the molecular weight range of 500 to 4 million g mol⁻¹ with high resolution. All samples were eluted at a flow rate of 1.0 mL min⁻¹. Calibration was performed using narrow molecular weight PSTY standards (PDI_{RI} ≤ 1.1) ranging from 500 to 2 million g mol⁻¹. Data acquisition was performed using Empower software, and molecular weights were calculated relative to polystyrene standards.

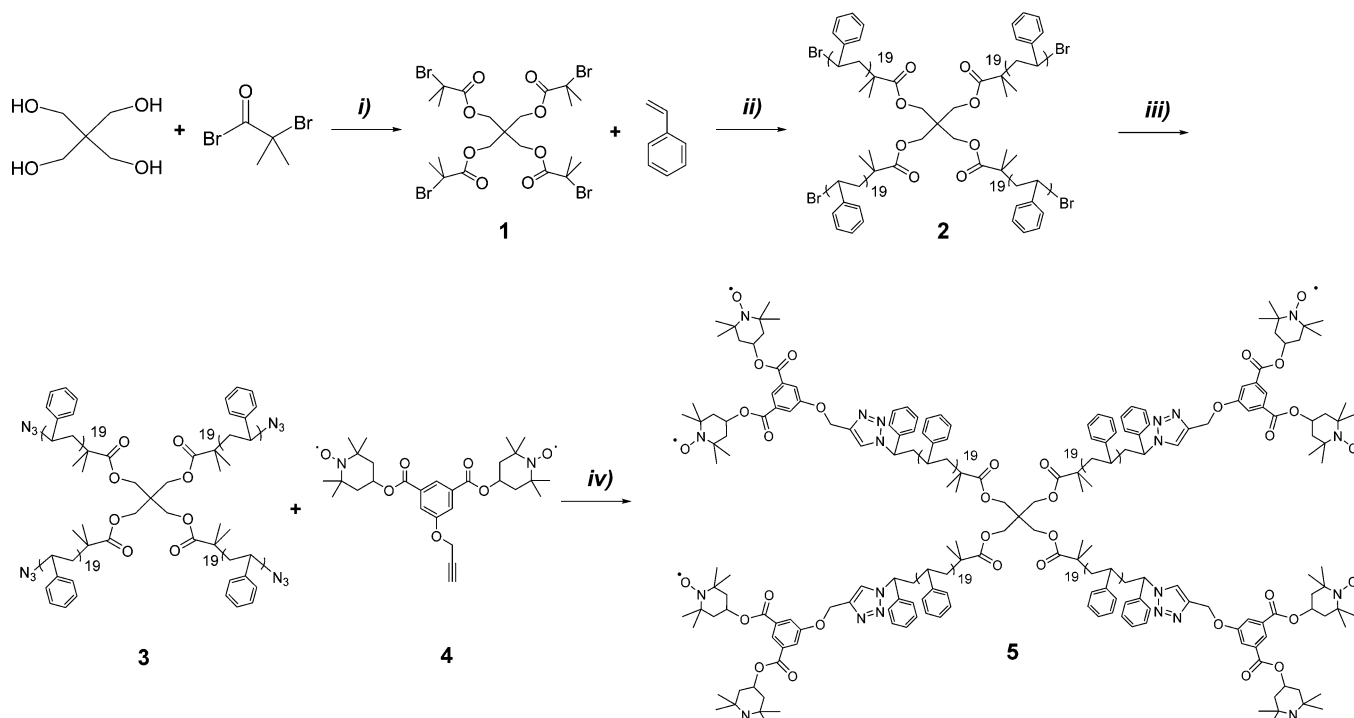
Absolute Molecular Weight Determination by Triple Detection SEC (TD-SEC). Absolute molecular weights of polymers were determined using a Polymer Laboratories GPC50 Plus equipped with dual angle laser light scattering detector, viscometer, and differential refractive index detector. HPLC grade *N,N*-dimethylacetamide (DMAc, containing 0.03 wt % LiCl) was used as the eluent at a flow rate of 1.0 mL min⁻¹. Separations were achieved using two PLGel Mixed B (7.8 × 300 mm) SEC columns connected in series and held at a constant temperature of 50 °C. The triple detection system was calibrated using a 2 mg mL⁻¹ PSTY standard (Polymer Laboratories: *M*_w = 110K, dn/dc = 0.16 mL g⁻¹, and IV = 0.5809). Samples of known concentration were freshly prepared in DMAc + 0.03 wt % LiCl and passed through a 0.45 μm PTFE syringe filter prior to injection. The absolute molecular weights and dn/dc values were determined using Polymer Laboratories Multi Cirrus software based on the quantitative mass recovery technique.

Preparative Size Exclusion Chromatography (Prep-SEC). Crude polymers were fractionated (i.e., purified) using a Varian Pro-Star preparative SEC system equipped with a manual injector, differential refractive index detector, and single wavelength ultraviolet visible detector. The flow rate was maintained at 10 mL min⁻¹, and HPLC grade THF was used as the eluent. Separations were achieved using a PL Gel 10 μm 10 × 10³ Å, 300 × 25 mm preparative SEC column at 25 °C. The dried crude polymer was dissolved in THF at 100 mg/mL and filtered through a 0.45 μm PTFE syringe filter prior to injection. Fractions were collected manually, and the composition of each was determined using the Polymer Laboratories GPC50 Plus equipped with triple detection as described above.

Nuclear Magnetic Resonance (NMR). All NMR spectra were recorded on either a Bruker DRX 400 or 500 MHz spectrometer using an external lock (CDCl₃), and all spectra were referenced to the residual nondeuterated solvent (CHCl₃). Spectra of functional molecules and polymers containing nitroxide radicals were measured in the presence of phenylhydrazine under an inert atmosphere to reduce the nitroxides to their incipient hydroxylamines.

Diffusion-Ordered Spectroscopy (DOSY) NMR. 1D DOSY experiments were run to suppress the solvent and organic peroxide (from THF) impurities, which appeared in ¹H NMR spectra of all polymers (including starting building blocks and dendrimers). A gradient strength (gpz6) of 85% (for starting building blocks) and 90% (for dendrimers), gradient pulse length (p30, little delta, δ = p30 × 2) 2 ms (for starting building blocks) and 2.5 ms (for dendrimers), and relaxation delay (*d*₁) 5 s (≥5*T*₁) with 256–512 scans were the parameters used in the 1D DOSY experiment.

2D DOSY experiments were carried out to determine the diffusion coefficients (*D*) for dendrimers (14, 15, and 16) in CDCl₃. All 2D DOSY experiments were conducted at 298 K at a dendrimer concentration of 10 mg mL⁻¹ in CDCl₃ using a Bruker Avance DRX 500 spectrometer operating at 500.13 MHz for protons and equipped with a 5 mm triple-resonance (¹H, ¹³C, ¹⁵N) *z*-gradient probe equipped with actively shielded gradients. The *z*-gradient was calibrated at 298 K with a HDO sample containing 0.1 mg mL⁻¹ GdCl₃. The maximum *z*-gradient amplitude was 50 G cm⁻¹. A 90° pulse calibration was performed for each new sample. A bipolar pulse longitudinal eddy current delay (BPPLD) pulse sequence was used. The pulse sequences included a 5 ms delay to allow residual eddy currents to decay. Sine-shaped gradient pulses were utilized to further minimize eddy currents. The gradient pulse length (p30, little delta, δ = p30 × 2) 2.5 ms was chosen for diffusion time in order to obtain the minimum residual signal for each component at maximum gradient strength. The diffusion delay (Δ) was set to 200 ms. The pulse gradients were incremented from 2 to 95% of the maximum gradient strength in a linear ramp (16 steps). A spectral window of 6000 Hz was accumulated in an acquisition time of 1.38 s. The relaxation time *T*₁ was determined by inversion recovery method. A relaxation delay of 5*T*₁ of the slowest relaxing signal was used (5 s). The FIDs were collected into 16K data points; 128 scans and 4 dummy scans were acquired on each sample. Following acquisition the FIDs were Fourier transformed applying zero-filling to 16K data points and an exponential window function with line broadening factor 1–5 Hz.

Scheme 2. Synthetic Route for Building Block 5 (4-Arm PSTY-(NO[•])₂)^a

^a(i): THF, TEA, 0 °C–RT, 6 h. (ii) CuBr, PMDETA, Cu(II)Br₂/PMDETA, anisole, 80 °C, 9 h. (iii) DMF, NaN₃, 25 °C, 24 h. (iv) CuBr, PMDETA, toluene, 25 °C, 1 h.

Data were processed using Bruker XWIN NMR software. The signal decay due to gradients was fitted using

$$I = I_0 \exp(-D\gamma^2 \delta^2 (\Delta - \delta/3)) \quad (1)$$

where I is the resonance intensity measured for a given gradient strength, I_0 is the signal intensity with no gradient applied, γ is the gyromagnetic ratio, δ is the gradient duration ($p30 \times 2$), and Δ is the diffusion delay. The resulting diffusion coefficients (D) of the polymer signals and the solvent are the result of the fitting procedure (see Supporting Information).

The hydrodynamic diameter ($D_{h,NMR}$) was determined using the Stokes–Einstein equation

$$D_h = 2R_h = \frac{kT}{3\pi\eta D} \quad (2)$$

where k is the Boltzmann constant ($1.380 \times 10^{-23} \text{ J K}^{-1}$), T is the temperature in kelvin (298 K), η is the viscosity of the solvent in pascal seconds ($5.3 \times 10^{-4} \text{ Pa s}$ for CDCl_3), and D is the diffusion coefficient obtained from 2D DOSY experiment.⁴⁴

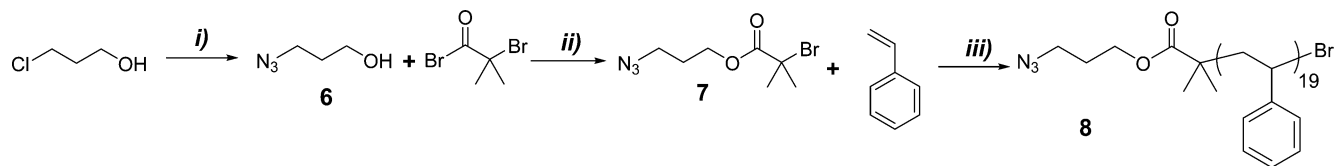
Attenuated Total Reflectance–Fourier Transform Spectroscopy (ATR-FTIR). ATR-FTIR spectra were obtained using a horizontal, single bounce, diamond ATR accessory on a Nicolet Nexus 870 FT-IR. Spectra were recorded between 4000 and 500 cm^{-1} for 32 scans at 4 cm^{-1} resolution with an OPD velocity of 0.6289 cm^{-1} . Solids were pressed directly onto the diamond internal reflection element of the ATR without further sample preparation.

Matrix-Assisted Laser Desorption Ionization–Time-of-Flight (MALDI-ToF) Mass Spectrometry. MALDI-ToF MS spectra were obtained using a Bruker MALDI-ToF autoflex III smart beam equipped with a nitrogen laser (337 nm, 200 Hz maximum firing rate) with a mass range of 600–400 000 Da. Spectra were recorded in either reflectron mode (1500–4500 Da) or linear mode (4000–20 000 Da). *trans*-2-[3-(4-*tert*-Butylphenyl)-2-methylpropenyldiene]-malononitrile (DCTB; 20 mg mL^{-1} in THF) was used as the matrix and $\text{Ag}(\text{CF}_3\text{COO})$ (1 mg mL^{-1} in THF) as the cation source for all the polystyrene samples. 20 μL of polymer solution (1 mg mL^{-1} in THF), 20 μL of DCTB solution, and 2 μL of $\text{Ag}(\text{CF}_3\text{COO})$ solution

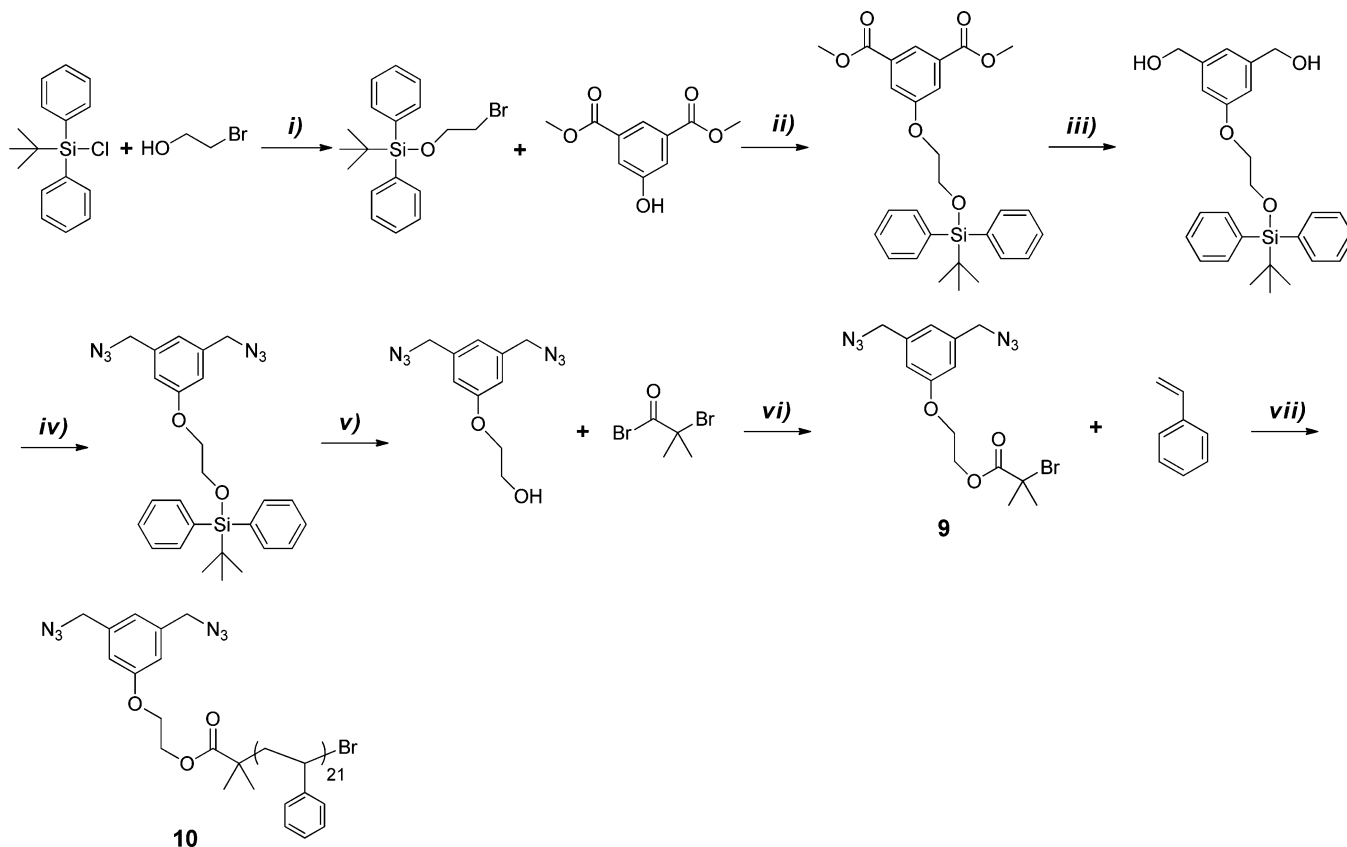
were mixed in an Eppendorf tube, vortexed, and centrifuged. 1 μL of solution was placed on the target plate spot, the solvent evaporated at ambient condition, and the measurement run. For lysine dendron 13, $\text{Na}(\text{CF}_3\text{COO})$ (1 mg mL^{-1} in THF) was used as cation source.

Synthesis of 4-Arm ATRP Initiator, 1. A solution containing 2-bromoisobutyryl bromide (25.1 g, 0.109 mol) dissolved in 80 mL of dry THF was added dropwise to another solution containing pentaerythritol (3.0 g, 2.2×10^{-2} mol) and triethylamine (11.1 g, 0.109 mol) dissolved in 220 mL of dry THF at 0 °C. The reaction was allowed to stir for 6 h and filtered to remove the salts, and then the filtrate concentrated by rotary evaporation. The product was dissolved in 300 mL of ether and sequentially washed with 10 wt % HCl, saturated NaHCO_3 solution, and brine. The organic layer was collected, dried over anhydrous MgSO_4 , and filtered. The filtrate was concentrated by rotary evaporation. The concentrate was purified by silica gel column chromatography using ethyl acetate/petroleum spirit (1/6, v/v) as the eluent. Product 1 was obtained as white crystals (10.65 g, 66.0%). R_f (1/6 EtOAc/petroleum spirit) 0.61. ¹H NMR (CDCl_3 , 298 K, 400 MHz): δ 1.92 (s, 24H, CH_3 –), 4.30 (s, 8H, $-\text{OCH}_2\text{C}-$). ¹³C NMR (CDCl_3 , 298 K, 400 MHz): 30.62, 43.64, 55.18, 62.88, 170.89.

Synthesis of Building Block 2 (4-Arm PSTY-Br). Freshly purified styrene (9.02 g, 8.66×10^{-2} mol), PMDETA (0.078 mL, 3.76×10^{-4} mol), 1 (0.254 g, 3.76×10^{-4} mol), anisole (10 mL), and $\text{Cu}(\text{II})\text{Br}_2/\text{PMDETA}$ (0.037 g, 9.41×10^{-5} mol) were added to a 20 mL Schlenk tube equipped with a magnetic stirrer and purged with argon for 20 min. $\text{Cu}(\text{I})\text{Br}$ (0.054 g, 3.77×10^{-4} mol) was carefully added under positive argon flow, and the reaction mixture was purged with argon for a further 5 min. The flask was placed in a temperature-controlled oil bath at 80 °C for 9 h. The reaction was stopped by quenching in ice and exposure to air. The polymerization mixture was diluted with DCM, and the copper salts were removed by passage through an activated basic alumina column. The solution was concentrated by rotary evaporation, and the polymer was recovered by precipitation into methanol, filtered, and dried for 48 h under high vacuum at 25 °C. The resultant polymer was precipitated from DCM into MeOH, filtered, and dried under high vacuum for 48 h at 25 °C

Scheme 3. Synthetic Route for Building Block 8^a

^a(i) NaI, NaN₃, DMSO/H₂O, 80 °C, 2 days. (ii) TEA, THF, 0 °C–RT, 6 h. (iii) CuBr, PMDETA, Cu(II)Br₂/PMDETA, bulk, 80 °C, 7.5 h.

Scheme 4. Synthetic Route for Building Block 10^a

^a(i) Imidazole, THF, 0 °C–RT, 12 h. (ii) 18-C-6, K₂CO₃, acetone, reflux, 48 h. (iii) LiAlH₄, THF, 0 °C–RT, 16 h. (iv) DPPA, DBU, toluene, 0 °C–RT, dark, 16 h. (v) TBAF, THF, argon, RT, 12 h. (vi) TEA, THF, 0 °C–RT, 12 h. (vii) CuBr, PMDETA, Cu(II)Br₂/PMDETA, bulk, 80 °C, 220 min.

give a white polymer, which was further purified by preparative SEC. The resultant polymer was reprecipitated from THF into MeOH, filtered, dried under high vacuum for 48 h at 25 °C, and obtained as peach powder ($M_{n,RI} = 8670$, $M_{p,RI} = 8710$, $PDI_{RI} = 1.05$, $M_{n,TD} = 9700$, $M_{p,TD} = 9840$, $PDI_{TD} = 1.02$, $M_{n,NMR} = 10\,820$, monomer conversion 39.0% as determined by gravimetric method).

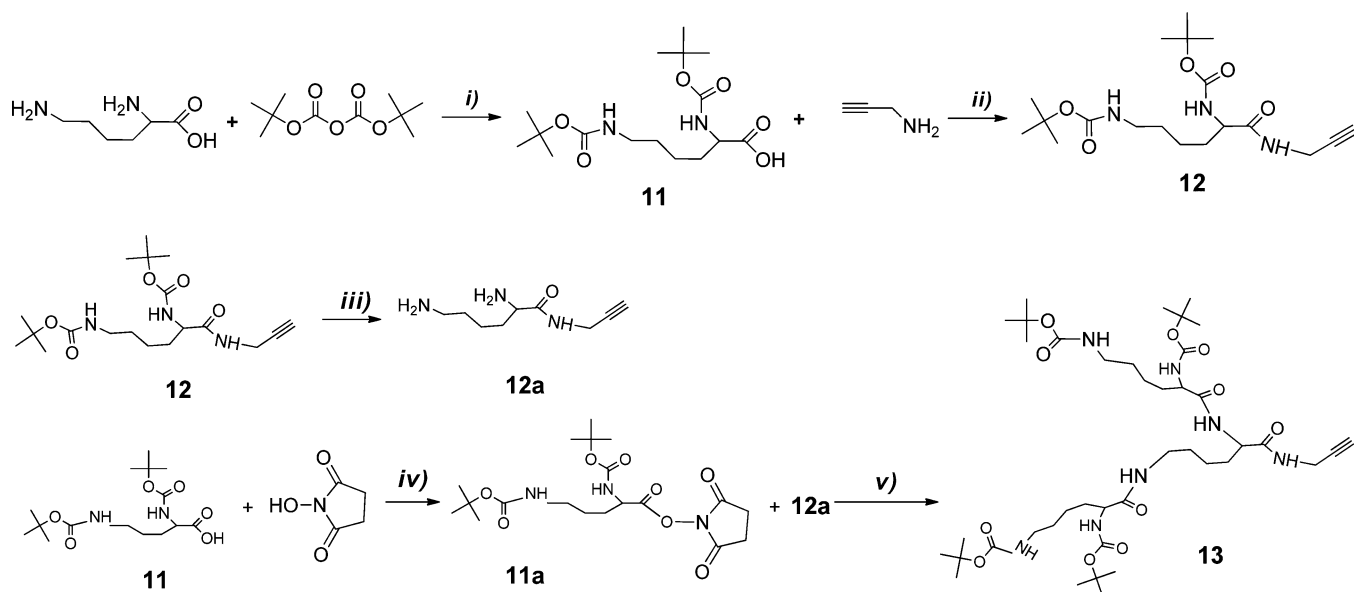
Synthesis of Building Block 3 (4-Arm PSTY-N₃). NaN₃ (0.34 g, 5.25×10^{-3} mol) was added to a stirred solution of **2** (1.16 g, 1.31×10^{-4} mol) in 6 mL of DMF. The reaction mixture was stirred for 24 h at room temperature. The polymer was twice precipitated into methanol (once from DMF, once from DCM), recovered by vacuum filtration and washed extensively with water and methanol. The polymer was dried under high vacuum for 48 h at 25 °C obtained as white powder ($M_{n,RI} = 8730$, $M_{p,RI} = 8810$, $PDI_{RI} = 1.05$, $M_{n,TD} = 9630$, $M_{p,TD} = 9790$, $PDI_{TD} = 1.02$, $M_{n,NMR} = 10\,670$).

Synthesis of 5 (4-Arm PSTY-(NO^{*})₂). The trifunctional linker, **4**, was synthesized according to the literature procedure.⁴⁰ In a 20 mL Schlenk tube, **4** (0.096 g, 1.82×10^{-4} mol) was added to a stirred solution of **3** (0.35 g, 4.04×10^{-5} mol) and PMDETA (7.0×10^{-3} g, 4.04×10^{-5} mol) in 6 mL of toluene. The reaction mixture was purged with argon for 15 min. Cu(I)Br (5.7×10^{-3} g, 4.04×10^{-5} mol) was

added to the solution under a positive flow of argon, sealed, and stirred for 1 h at 25 °C. The polymer was diluted with DCM, and the copper salts were removed by passage through an activated basic alumina column. The solution was concentrated by rotary evaporation, and the polymer was recovered by two precipitations (once from toluene and once from DCM) into methanol, collected by vacuum filtration, and washed extensively with methanol. The polymer was dried under high vacuum for 48 h at 25 °C to give a peach-colored polymer. The resultant polymer was reprecipitated from THF into MeOH, filtered, and dried under high vacuum for 48 h at 25 °C and obtained as peach powder ($M_{n,RI} = 10\,200$, $M_{p,RI} = 10\,320$, $PDI_{RI} = 1.04$, $M_{n,TD} = 11\,600$, $M_{p,TD} = 11\,760$, $PDI_{TD} = 1.01$, $M_{n,NMR} = 12\,640$).

Synthesis of Building Block N₃-PSTY-Br 8. The ATRP initiator **7** (Scheme 3) was synthesized according to the literature procedure.⁴² The synthetic strategies to produce **7** and **8** are given in Supporting Information (8, $M_{n,RI} = 2370$, $M_{p,RI} = 2490$, $PDI = 1.08$, $M_{n,NMR} = 2870$, monomer conversion 47.6% as determined by gravimetry).

Synthesis of Building Block 10. The ATRP initiator **9** was synthesized according to the literature procedure.¹⁹ The synthetic strategies to produce **9** and **10** are given in Supporting Information

Scheme 5. Synthesis of Alk-Lysine-Boc (12) and Alk-Lysine-Boc Dendron (13)^a

^a(i) NaOH, H₂O, 1,4-dioxane, 0 °C–RT, 7 h. (ii) DCC, DMAP, DCM, 0 °C–RT, 24 h. (iii) TFA, DCM, RT, 2 h. (iv) DCM, DCC, NHS, 0 °C–RT, 2 h. (v) DMF, TEA, RT, 12 h.

(10, $M_{n,RI} = 2600$, $M_{p,RI} = 2690$, PDI = 1.07, $M_{n,NMR} = 2830$, monomer conversion 46.9% as determined by gravimetry).

Synthesis of Building Block 12 (Alkyne-Lysine-Boc). The Boc-Lysine-OH, **11**, was synthesized according to ref 43 (Scheme 5). To a 500 mL flask, **11** (6.0 g, 0.172 mol), propargylamine (1.90 g, 0.0345 mol), and DMAP (0.316 g, 2.59×10^{-3} mol) were dissolved in 120 mL of dry DCM and cooled to 0 °C in an ice bath. A mixture of DCC and 50 mL of DCM was added dropwise into the solution over 30 min. The mixture was allowed to react for 36 h at room temperature. The solid content was removed by filtration, and the filtrate was washed by saturated brine (2×50 mL). The organic layer was collected, dried over anhydrous MgSO₄, and the solvent removed *in vacuo* followed by column chromatography using ethyl acetate/petroleum spirit (3/1, v/v) as the eluent. Product **12** was obtained as a white solid (2.86 g, yield = 41.7%). R_f (3/1 EtOAc/petroleum spirit) 0.65. ¹H NMR (CDCl₃, 298 K, 500 MHz): δ 6.91 (s, 1H, CHCCH₂NHCO–), 5.32 (s, 1H, –CHNHCO–), 4.69 (s, 1H, –CH₂NHCO), 3.97–4.07 (b, 3H, CH₂CCH₂NH– and –CH₂CHCO–), 3.08 (t, 2H, $J = 6.6$ Hz, –CH₂CH₂NH–), 2.20 (t, 1H, $J = 2.5$ Hz, HCCCCH₂–), 1.2–2.0 (m, 24H, CH₂-Lys and CH₃-Boc). ¹³C NMR (CDCl₃, 298 K, 500 MHz): 22.69, 28.44, 28.53, 29.09, 29.70, 32.23, 40.07, 54.24, 71.60, 79.16, 79.53, 80.10, 155.97, 156.26, 172.22.

Synthesis of Alkyne-Lysine-Boc Dendron (13). **11** (2.25 g, 6.51×10^{-3} mol), NHS (1.5 g, 0.013 mol), and DCC (2.63 g, 0.013 mol) were dissolved in 50 mL of DCM, which was cooled to 0 °C in an ice bath. The reaction mixture was heated to room temperature and stirred for 2 h; the solid was filtered, the filtrate was evaporated, and the concentrate, **11a**, was dissolved in 20 mL of DMF and used without further purification. **12** (1.12 g, 2.93×10^{-3} mol) was dissolved in 6 mL of TFA/DCM mixture (1:1, v/v), stirred for 2 h, and the solvent evaporated. The concentrate, **12a**, was dissolved in 20 mL of DMF and then added dropwise into the 20 mL DMF/**11a** mixture above over 20 min. The mixture was stirred for another 12 h. The reaction mixture was then concentrated. The concentrate was dissolved in 200 mL of DCM and washed sequentially with 10 wt % HCl solution, saturated NaHCO₃ solution, and brine. The organic layer was collected, dried over anhydrous MgSO₄, and filtered. The filtrate was concentrated by rotary evaporation. The concentrate was purified by silica gel column chromatography using 100% EtOAc as the eluent. Product **13** was obtained as white solid (1.4 g, yield =

56.9%). R_f (100% EtOAc) 0.51. MALDI-ToF MS: $[M + Na^+]$ Calcd = 862.52, Found = 862.89. $[M + K^+]$ Calcd = 878.50, Found = 878.72.

Synthesis of Dendrimer 14 in a One-Pot Reaction. In a 10 mL Schlenk tube, **5** (90.0 mg, 7.76×10^{-6} mol), **8** (156 mg, 6.51×10^{-5} mol), **12** (48.0 mg, 1.24×10^{-4} mol), and PMDETA (20 μ L, 9.31×10^{-5} mol) were dissolved in 2 mL of toluene and 2 mL of DMSO. The reaction mixture was then purged with argon for 30 min. Cu(I)Br (13.5 mg, 9.31×10^{-5} mol) was added to the solution under a positive flow of argon, sealed, and stirred for 30 min at 25 °C in a temperature-controlled oil bath. The polymer was diluted with DCM, and the copper salts were removed by passage through an activated basic alumina column. The solution was concentrated by rotary evaporation and the polymer recovered by precipitation into methanol, collected by vacuum filtration, and washed extensively with methanol. The polymer was dried under high vacuum for 48 h at 25 °C to give a white polymer and further purified by preparative SEC. The resultant polymer was reprecipitated from DCM into MeOH, filtered, and dried under high vacuum for 48 h at 25 °C and obtained as white powder ($M_{n,RI} = 26$ 590, $M_{p,RI} = 27$ 650, PDI = 1.08; $M_{n,TD} = 35$ 120, $M_{p,TD} = 35$ 990, PDI = 1.05, $M_{n,NMR} = 39$ 340).

Synthesis of Dendrimer 15 in a One-Pot Reaction. In a 10 mL Schlenk tube, **5** (90.0 mg, 7.76×10^{-6} mol), **10** (171 mg, 6.51×10^{-5} mol), **12** (71.9 mg, 1.86×10^{-4} mol), and PMDETA (26 μ L, 1.24×10^{-4} mol) were dissolved in 1 mL of toluene. The reaction mixture was then purged with argon for 15 min. Cu(I)Br (18 mg, 1.24×10^{-4} mol) was then added to the solution under a positive flow of argon, sealed, and stirred for 30 min at 25 °C in a temperature-controlled oil bath. The polymer was diluted with DCM, and the copper salts were removed by passage through an activated basic alumina column. The solution was concentrated by rotary evaporation, and the polymer was recovered by precipitation into methanol, collected by vacuum filtration, and washed extensively with methanol. The polymer was dried under high vacuum for 48 h at 25 °C to give a white polymer and further purified by preparative SEC. The resultant polymer was then reprecipitated from DCM into MeOH, filtered, dried under high vacuum for 48 h at 25 °C, and obtained as white powder ($M_{n,RI} = 29$ 140, $M_{p,RI} = 30$ 520, PDI = 1.08; $M_{n,TD} = 37$ 540, $M_{p,TD} = 38$ 590, PDI = 1.05, $M_{n,NMR} = 43$ 990).

Synthesis of Dendrimer 16 in a One-Pot Reaction. In a 10 mL Schlenk tube, **5** (90.0 mg, 7.76×10^{-6} mol), **10** (171 mg, 6.51×10^{-5} mol), **13** (160 mg, 1.86×10^{-4} mol), and PMDETA (26 μ L, 1.24×10^{-4} mol) were dissolved in 1 mL of toluene. The reaction mixture

was then purged with argon for 15 min. Cu(I)Br (18 mg, 1.24×10^{-4} mol) was then added to the solution under a positive flow of argon, sealed, and stirred for 30 min at 25 °C in a temperature-controlled oil bath. The polymer was diluted with DCM, and the copper salts were removed by passage through an activated basic alumina column. The solution was concentrated by rotary evaporation, and the polymer was recovered by precipitation into methanol, collected by vacuum filtration, and washed extensively with methanol. The polymer was dried under high vacuum for 48 h at 25 °C to give a white solid and further purified by preparative SEC. The resultant polymer was then reprecipitated from DCM into MeOH, filtered, and dried under high vacuum for 48 h at 25 °C obtained as a white powder ($M_{n,RI} = 31\,200$, $M_{p,RI} = 33\,360$, PDI = 1.08; $M_{n,TD} = 45\,640$, $M_{p,TD} = 46\,330$, PDI = 1.03, $M_{n,NMR} = 53\,540$).

Deprotection of Boc Groups from Boc-Lysine Units of Dendrimer. Typically, dendrimer (30 mg) was dissolved in a mixture of DCM (1 mL) and TFA (1 mL). The solution was kept stirring for 12 h at room temperature, the solvent was removed by evaporation, and the residual content was dried in high vacuum for 24 h. The resulting product was used for further micellization in water directly.

Micellization of Dendrimers. Typically, 5 mg of dendrimer (after deprotection of the Boc groups) was dissolved in 3 mL of DMF (a common solvent for both PSTY and Lysine units) followed by the gradual addition (at a rate of $0.013 \text{ mL min}^{-1}$) of 3 mL of water (a nonsolvent for the hydrophobic PSTY blocks). The resulting mixture of DMF and water was transferred to presoaked and rinsed dialysis bag (Pierce Snakeskin, MWCO 3.5K) and dialyzed against a large volume of Milli-Q water for 2 days to remove the organic solvent. After dialysis, additional water was then added to the water solution to make up 10 mL. This ensured that the final concentration of the dendrimers was 0.5 mg mL^{-1} . It should be noted that a small amount of precipitant was observed after the self-assembly of 17, thereby slightly reducing its concentration.

Dynamic Light Scattering (DLS). Dynamic light scattering measurements were performed using a Malvern Zetasizer Nano Series running DTS software and operating a 4 mW He–Ne laser at 633 nm. Analysis was performed at an angle of 173° and a constant temperature of 25 °C. The hydrodynamic diameter of dendrimer before the removal of Boc groups from Boc-Lysine units was measured in CDCl_3 (5 mg mL^{-1}). The hydrodynamic diameter and zeta potential of dendrimer after the removal of Boc groups was measured in water (0.5 mg mL^{-1} , micelle solution). All the samples were filtered by $0.45 \mu\text{m}$ filter before measurements. The number-average hydrodynamic particle size, polydispersity index, and zeta potential are reported. The polydispersity index (PDI) was used to describe the width of the particle size distribution. It was calculated from a Cumulants analysis of the DLS measured intensity autocorrelation function and is related to the standard deviation of the hypothetical Gaussian distribution (i.e., $\text{PDI}_{\text{PSD}} = \sigma^2/Z_D^2$, where σ is the standard deviation and Z_D is the Z average mean size).

Transmission Electron Microscopy (TEM). The samples for TEM analysis were prepared by placing a drop of the micelle solution (0.5 mg mL^{-1}) of dendrimer onto a Formvar-precoated copper TEM support grid and allowed to air-dry before measurement. The micelles were characterized on a Jeol-1010 instrument utilizing an accelerating voltage of 80 kV at ambient temperature.

LND Simulations. We used a log-normal distribution (LND) model based on a Gaussian function to fit the experimental MWD. One can simulate the molecular weight distributions, and in particular the weight distribution,⁴⁵ with a log-normal distribution (see ref⁴⁶ for more details) using the following equations:

$$w(M) = \frac{\exp(-(\ln M - \ln \bar{M})^2 / 2\sigma^2)}{M(2\pi\sigma^2)^{0.5}} \quad (3)$$

where

$$\bar{M} = (M_n M_w)^{0.5} \quad (4)$$

and

$$\sigma^2 = \ln(\text{PDI}) \quad (5)$$

where eq 1 is the Gaussian distribution function of $w(M)$ (the weight distribution of the SEC trace), M_n is the number-average molecular weight, M_w is the weight-average molecular weight, and the polydispersity $\text{PDI} = M_w/M_n$.

RESULTS AND DISCUSSION

Synthesis of Building Blocks. The synthesis of a 4-arm polystyrene star (2) by ATRP using a tetrafunctional bromine initiator, 1 (see synthesis and characterization in Supporting Information and ¹H NMR in Figure S1), is given in Scheme 2. The produced 4-arm star exhibited a narrow molecular weight distribution (MWD) with an $M_{n,RI}$ of 9140 and polydispersity index (PDI) of 1.09. The SEC trace (i.e., weight distribution) of 2 (crude, curve a) given in Figure 1 showed a high molecular

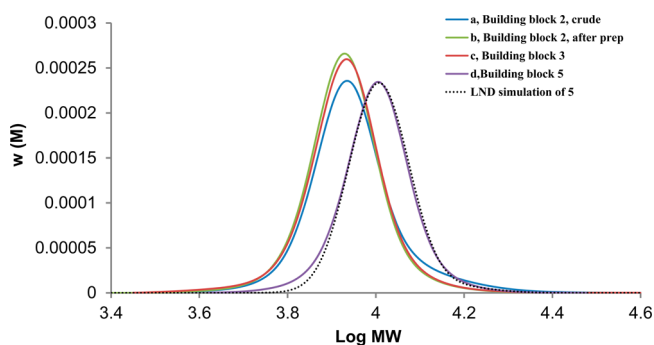


Figure 1. Molecular weight distributions (MWDs) for starting polymer (2 and 3) and product (5) obtained from SEC-RI based on a polystyrene calibration curve: (a) 4-arm PSTY-Br (2 crude), (b) 4-arm PSTY-Br (2 after prep), (c) 4-arm PSTY- N_3 (3), (d) 4-arm PSTY- $(\text{NO})_2$ (5). Dotted line represents the LND fit to 5. All SEC traces were normalized to weight.

weight tail most likely the result of star–star coupling, which was removed by preparative SEC (i.e., 2 after prep, curve b). The purity of the 4-arm star (2 crude) relative to the higher molecular weight species formed through star–star radical coupling was determined by simulating the weight distributions from SEC based on a log-normal distribution (model) using a Gaussian function (Figure S2 and Table S1 in Supporting Information). The purity of the crude 4-arm star was 87.3%, which increased to 96.1% after purification by preparative SEC (Table 1). In addition, the chain-end functionality of 2 after preparative SEC was 98% determined by ¹H NMR (Figure 2A), and from the MALDI-ToF (Figure 3A) the only species detected was the chain-end fragmentation with added Ag^+ (e.g., m/z found was 9266.20, which was close to that calculated 9266.37). These results suggested that this 4-arm star would provide a suitable core building block to produce the final dendrimers in high yields.

Azidation of the bromine groups on 2 (i.e., after purification) to produce 3 showed a distinct shift of the proton adjacent to the azide from ~ 4.5 to 4 ppm (Figure 2), a slight increase in the $M_{n,RI}$ value (Table 1), and the near-quantitative conversion further confirmed by analysis of the MALDI (Figure 3B) spectrum. The SEC trace of 3 (i.e., 2 after azidation) was nearly identical to that of 2 (after prep) as shown in Figure 1. The trifunctional linker, 4, consisted of an alkyne and two nitroxide moieties (see Scheme 2), with its characterization given in the Supporting Information (Figures S4–S6). Coupling 3 and 4 using the CuAAC reaction resulted in a slight shift of the MWD

Table 1. SEC and NMR Data for All Building Blocks

polymer	$M_{n,RI}^a$	$M_{p,RI}^a$	PDI	$M_{n,TD}^b$	$M_{p,TD}^b$	PDI ^f	$M_{n,theo}^g$	ΔHDV^c	$M_{n,NMR}$	chain-end functionality (%) ^d	purity ⁱ
2	9140	8730	1.09								87.3
2 ^e	8670	8710	1.05	9700	9840	1.02		0.89	10820	98.0	96.1
3	8730	8810	1.05	9630	9790	1.02	9550 ^g	0.90	10670	98.0	94.9
5	10200	10310	1.04	11600	11760	1.01	11660 ^g	0.88	12640	96.0	96.0
8	2500	2570	1.11								95.4
8 ^e	2370	2490	1.08				2480 ^h		2870	99.0	99.0
10	2600	2690	1.07				2820 ^h		2830	96.0	97.9

^aSEC (RI detector) was based on a PSTY calibration curve. ^bMWD determined from DMAc triple detection SEC. ^cHydrodynamic volume change ($\Delta HDV = M_{p,RI}/M_{n,TD}$). ^dChain-end functionality calculated from ¹H NMR. ^ePolymers fractionated (purified) by preparative SEC. ^fUnderestimation of true PDI value as light scattering has less sensitivity to low molecular weights. ^g $M_{n,theo}$ determined from $M_{n,TD}$ of 2 (after prep) plus the M_w of functional groups. ^h $M_{n,theo}$ determined by $M_{n,theo} = ([M]/[I]) \cdot M_n \cdot \text{con\%} + M_i$, where $[M]$, $[I]$, M_n , con\% , and M_i are the monomer concentration, initiator concentration, molecular weight of monomer, monomer conversion, and molecular weight of initiator, respectively. ⁱDetermined from log-normal distributions(LND) simulation.

to the expected molecular weight to produce 5 (Scheme 1). The 4-arm star 5 consisted of eight free nitroxides on its periphery. The MALDI-ToF given in Figure 3C showed that the peaks corresponded to the expected nitroxide end-functionalized 5 (e.g., m/z found was 12 593.38, which was close to 12 593.20 calculated with Ag^+), in agreement with the MALDI analysis of the previously synthesized polymers with nitroxide chain-end functionality.¹⁹ The ¹H NMR of the free nitroxides on 5 led to line broadening and poor resolution, whereas converting these nitroxides to hydroxylamines allowed us to obtain accurate NMR spectra. The ¹H NMR of 5, in which the nitroxides have been converted to hydroxylamines, showed near complete loss of the proton associated with the azide and presence of peaks at 5.1, 5.3, 7.8, and 8.2 ppm associated with peaks d, e, f, and g from the coupling reaction to produce 5 (Figure 2C). It was also found that the absolute $M_{n,TD}$ (11 600) was close to that calculated (11 660) from the addition of all the end-groups to the 4-arm star (Table 1).

The ATRP of initiator 7 with styrene (Scheme 3) gave telechelic polymer 8 (crude) with approximately 4.6 wt % of double molecular weight polymer formed through radical-radical coupling (see Figure S10 and Table S2 in Supporting Information). After purification by preparative SEC, its purity increased to 99.0% (Figure S10 and Table S2) and chain-end functionality was close to 99% as determined by ¹H NMR (Figure 4A) from the near 4:1 ratio of proton e to that of a and c. Telechelic polymer 10 (Scheme 4), with a diazide functionality on one chain-end and a bromine on the other, was formed again using ATRP. As determined by the LND simulations, it showed greater than 97.9% purity (Figure S13 and Table S3) and approximately 96% chain-end functionality by ¹H NMR (Figure 4B) as given in Table 1, and thus 10 was used without further purification by preparative SEC. The high purity of both 8 and 10 was further supported by the MALDI analysis in Figures S11 and S14 in the Supporting Information. The other two building blocks 12 and 13 (see Scheme 1) consisted of Boc protected L-lysine groups. The synthetic strategy to make 12 and 13 is shown in Scheme 5. The amidation of 11 and propargylamine afforded 12 in a good yield of 41.7%. The Boc protected L-lysine dendron 13 formed through the reaction of 11a and 12a to give a yield of 56.9%. Characterization of 12 and 13 is given in Supporting Information (Figures S16–S22).

One-Pot Synthesis of Boc Protected L-Lysine Decorated Polymeric Dendrimers. Modulating the catalytic activity of copper for the orthogonal “click”-type reactions of

NRC and CuAAC produced third- or fourth-generational layer dendrimers coated on the periphery with L-lysine in one pot at 25 °C (Scheme 1). The NRC process occurs through the reaction of a nitroxide and a free radical to form an alkoxyamine.^{47,48} A method to produce radicals rapidly *in situ* employed the abstraction of the halide from the polymer end group with either Cu(I) or Cu(0).⁴⁷ It was found that in DMSO Cu(I)Br/Me₆TREN was highly reactive, rapidly producing radicals that were subsequently trapped by nitroxides to form the resultant alkoxyamines with little or no radical-radical coupling product.⁴⁸ As a solvent, DMSO has also been demonstrated to induce disproportionation of Cu(I)Br/Me₆TREN to the highly active Cu(0) and Cu(II) species.⁴⁹ Recent results showed that in DMSO, the NRC reaction was rapid and complete within less than 2 min.^{19,40} By changing the ligand to PMDETA and the solvent to toluene, the NRC reaction slowed significantly with coupling times greater than 2 h. Copper also catalyzes the CuAAC reaction. The coupling reaction using Cu(I)Br/PMDETA in toluene, in contrast to the NRC reaction, was rapid with complete coupling in less than 2 min. Conversely, using Cu(I)Br/Me₆TREN in DMSO slowed the CuAAC reaction with complete coupling in more than 30 min. However, using Cu(I)Br/PMDETA in a mixture of toluene and DMSO (50:50 v/v %) allowed the NRC and CuAAC reactions to proceed with similar rates of coupling. This latter method should produce the dendrimer much faster than in the other two solvent/ligand conditions.⁵⁰

Polymeric dendrimer 14 formed through the orthogonal NRC and CuAAC “click” reactions of 5, 8, and 12 in a molar ratio of 1:8.4:16 (Scheme 1), respectively, utilizing an excess of reactants 8 and 12 to the core 5. The parallel process using CuBr/PMDETA in a solvent mixture of toluene and DMSO (50:50 v/v %) produced 14 (crude) in 30 min at 25 °C. The SEC trace in Figure 5A showed that all core 5 (blue dotted line) was consumed and that the MWD contained the remaining excess of 8 (green dotted line) and 12 (orange dotted line). We determined a purity of 79 wt % from a fit of the theoretical MWD of 14, denoted as “LND (14, pure)” in Figure 5A by the black dotted line calculated from the addition of molecular weight of all arms to the core using a change in hydrodynamic volume (ΔHDV) of 0.77 in the LND method. Polymeric dendrimer 14 was then purified by preparative SEC to remove all starting reagents and other low molecular weight coupled products. After preparative SEC (see Figure 5A), the purity of 14 (after prep) determined by the LND method was 94% based on the fit of the theoretical MWD of 14. The 6% of

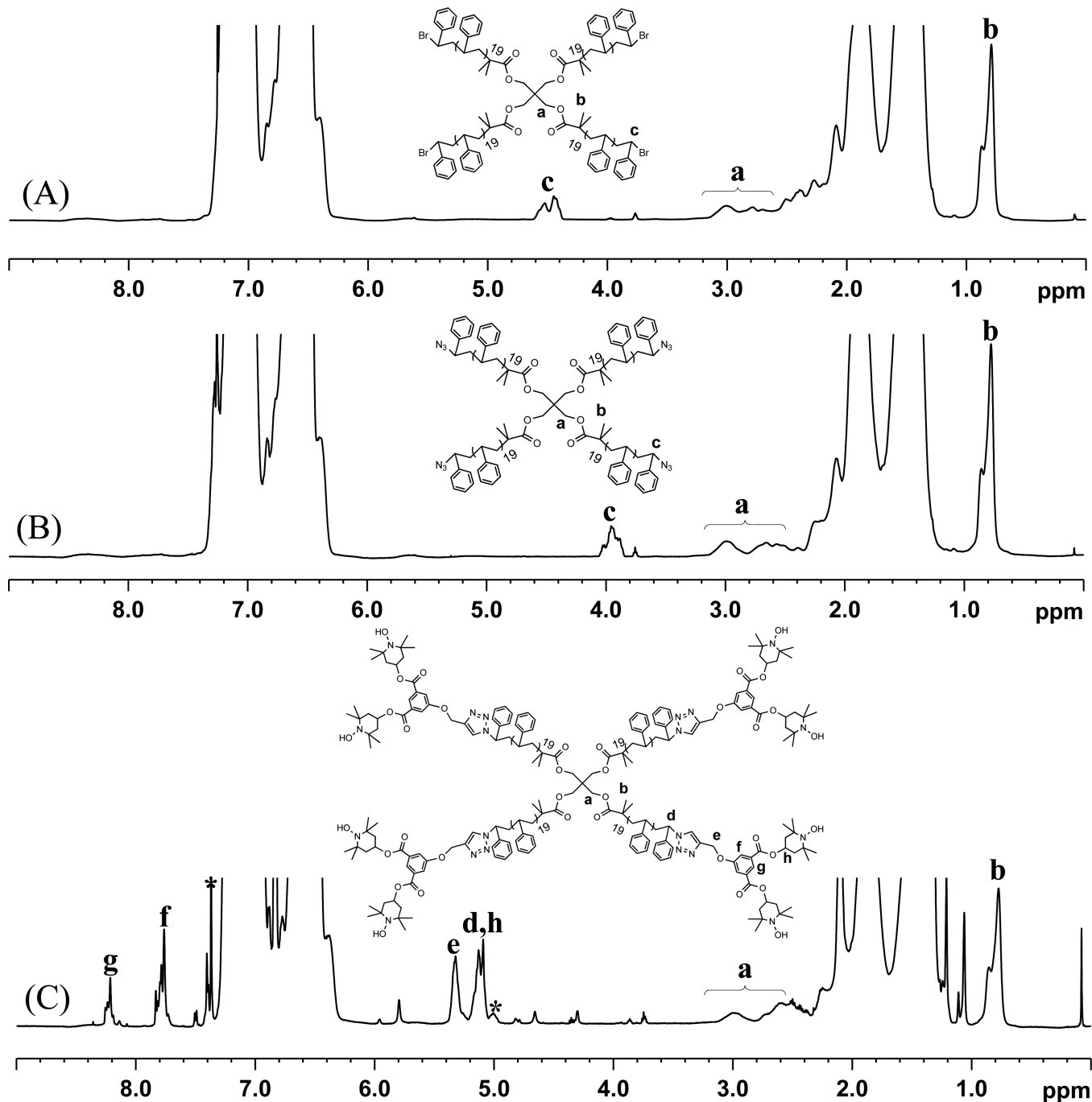


Figure 2. Comparison of ¹H 1D DOSY NMR spectra of (A) 4-arm PSTY-Br (2), (B) 4-arm PSTY-N₃ (3), and (C) 4-arm PSTY-(NO*)₂ (5). Recorded in CDCl₃, 298 K, 500 MHz, gradient strength (gpz6) 85%, gradient pulse length (p30) 2.0 ms. *Residual phenylhydrazine.

byproducts most probably results from the nonfully coupled L-lysine–alkyne to the polymeric dendrimer. The $M_{n,RI}$ of **14** (prep) was 26 590 with a PDI of 1.08 using the refractive index (RI) detector, and the $M_{n,TD}$ was 35 120 with a PDI of 1.05 using triple detection (i.e., absolute molecular weight determination) as given in Table 2. The value of $M_{n,TD}$ determined by triple detection was close to the theoretical value (33 640) of the dendrimer calculated from the addition of the absolute molecular weights of the building blocks (**5**, **8**, and **12**). It should be noted that the PDI from triple detection SEC was always lower due to a lower sensitivity of the light scattering at lower molecular weights. The change in ΔHDV from $M_{p,RI}$ to $M_{p,TD}$ of 0.77 was the same as that used in the

LND method above, supporting the calculated high purity of 94%. The lower apparent molecular weight (i.e., ΔHDV of 0.77) suggested that the polymeric dendrimer was much more compact than its corresponding linear analogue as a result of the many tethering links in each generational layer. Each link will reduce the amount of solvent required to swell the polymer arms.⁵¹ Further support for the high purity comes from analysis of the ¹H NMR (see Figure 6A and Figure S23) from integration of peaks corresponding to the three building blocks. Table 2 shows that the ratio of the number of arms in each generational layer was 4:8.2:8 and close to theory (4:8:8).

The next polymeric dendrimer synthesized was **15** with double the number of L-lysine on the periphery (Scheme 1).

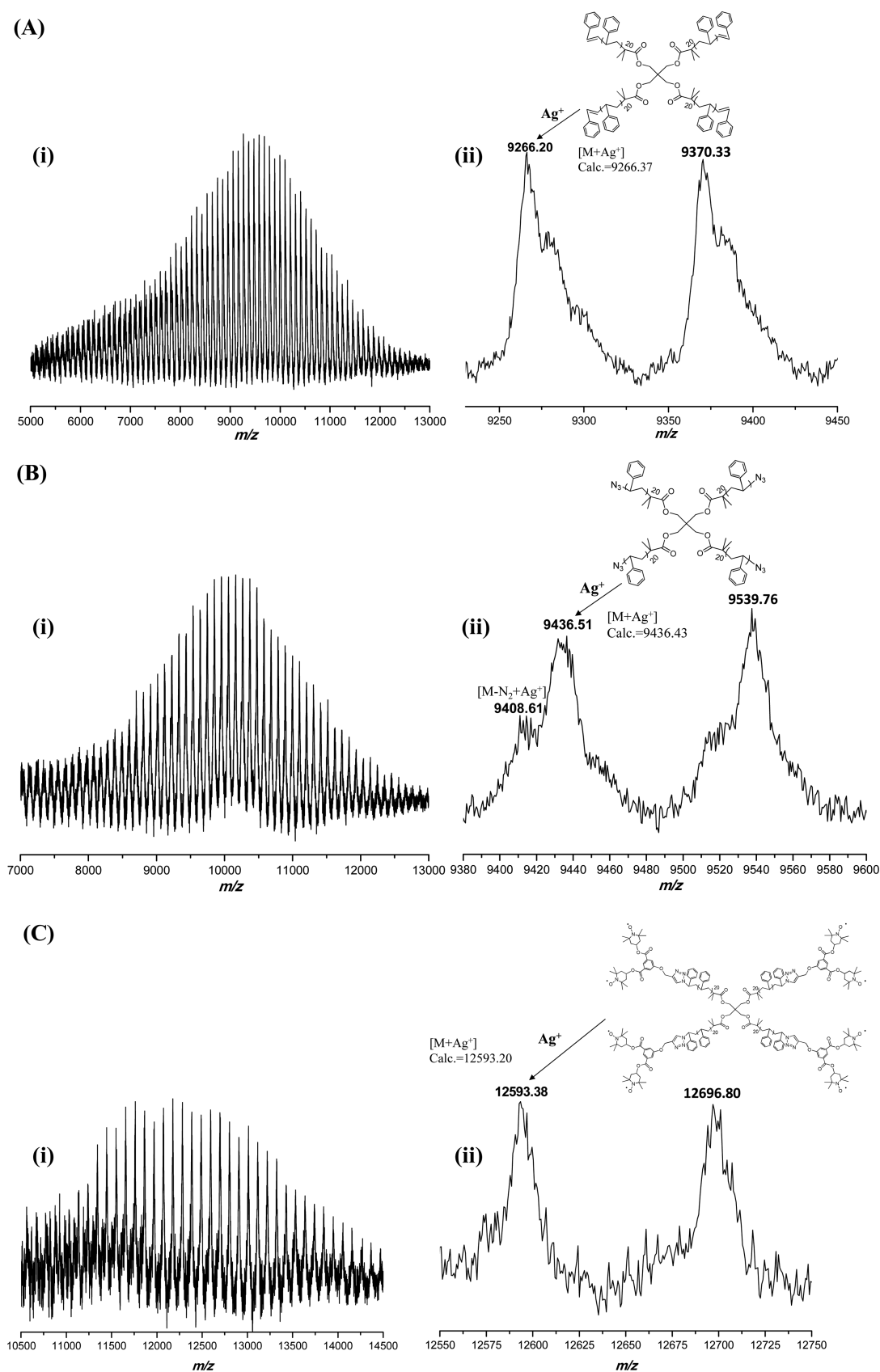


Figure 3. MALDI-TOF mass spectra of (A) 4-arm PSTY-Br (**2**), (B) 4-arm PSTY- N_3 (**3**), and (C) 4-arm PSTY- $(NO^*)_2$ (**5**). The spectra were recorded in linear mode using DCTB as the matrix and $Ag(CF_3COO)$ as the cation source: (i) full spectra and (ii) expanded spectra.

The molar ratio of starting reagents **5**, **10**, and **12** was 1:8.4:24 and using the same reaction conditions as those to produce **14**.

The SEC trace showed that **15** was produced (Figure 5B) with near complete loss of starting polymer **5** and remaining excess

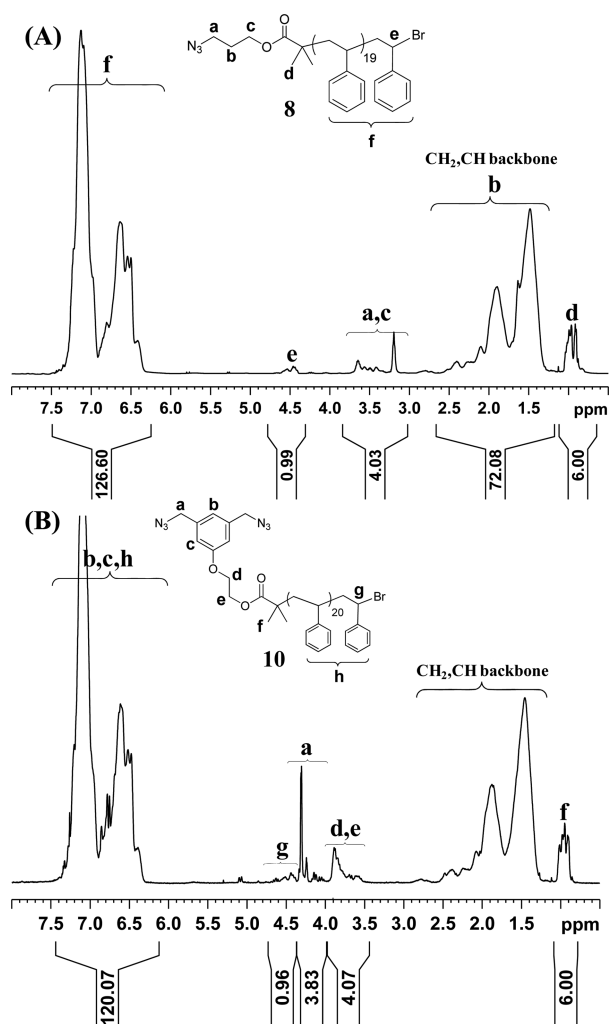


Figure 4. 1H 1D DOSY NMR spectra of (A) N_3 -PSTY-Br (**8**) and (B) $(N_3)_2$ -PSTY-Br (**10**) recorded in $CDCl_3$ at 298 K, 500 MHz, gradient strength (gpz6) 85%, gradient pulse length (p30) 2.0 ms; the sample **8** was purified by preparative-SEC.

of reactants **10** and **12**. The SEC trace showed products corresponding to the coupling of **10** and **12** through the CuAAC reaction. The purity of **15** (crude) was 74% determined by the LND method using the theoretical molecular weight of **15** and a ΔHDV of 0.76 (Figure 5B). After fractionation of **15** (crude) by preparative SEC, the purity increased to 96%. The $M_{n,RI}$ and PDI were 29 140 and 1.07, and the $M_{n,TD}$ and PDI by triple detection was 37 540 and 1.05, respectively (Table 2). The value of $M_{n,TD}$ (38 590) was close to the theoretical value (38 530) of the dendrimer calculated from the absolute molecular weight of the building blocks (**5**, **10**, and **12**). In addition, the ΔHDV determined from the ratio of $M_{p,RI}$ to $M_{p,TD}$ was 0.79, which was close to that used in the LND method above for **15** (crude). Analysis by 1H NMR (Figure 6B and Figure S24) gave the number of arms in each generational layer as equal to 4:8.1:16, which was very close to expected for a polymeric dendrimer to form **15**.

One of the main goals of this work was to create a dendrimer with a densely coated L-lysine periphery (i.e., with 32 lysine groups on the periphery and 16 lysine groups as the penultimate generational layer) as shown in Scheme 1. To do this, we produced a small molecule L-lysine dendron **13** with an alkyne end-functionality that was then coupled to **10** and **5** to

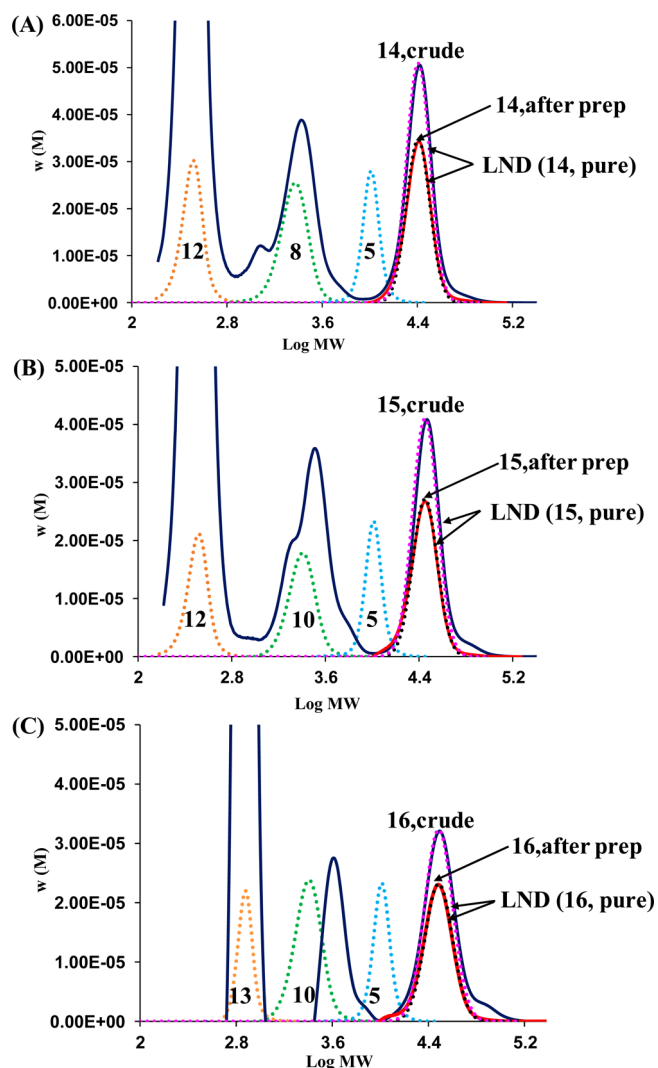


Figure 5. SEC traces of starting building blocks (**5**, **8**, **10**, **12**, **13**; dotted lines) to produce the respective dendrimers. Dendrimers before (crude, dark blue solid line) and after purification by preparative SEC (after prep, red solid line). All SEC traces were determined by THF SEC (RI). (A) Dendrimer **14** and LND simulation of pure (theoretical, dotted lines) **14**. (B) Dendrimer **15** and LND simulation of pure (theoretical, dotted lines) **15**. (C) Dendrimer **16** and LND simulation of pure (theoretical, dotted lines) **16**.

produce a fourth-generation layered (G4) polymeric dendrimer **16**. The molar ratio of starting reagents **5**, **10**, and **13** was 1:8.4:24, and using the same reaction conditions as for the previously made **14** and **15**. The MWD after the reaction showed a loss of reactants **5** and **10**, with new MWD peaks appearing that corresponded to the coupling of **10** and **13** and the final polymeric dendrimer **16**. There was still a large peak corresponding to the starting dendron **13**, which was used in large excess. The purity of the crude product **16** was lower (69%) compared to both **14** and **15** using a ΔHDV of 0.70 in the LND simulation (Figure 5C). Purification using preparative SEC gave an $M_{n,RI}$ of 31 200 (PDI = 1.08) and $M_{n,TD}$ of 45 640 (PDI = 1.03), in which the value of $M_{n,TD}$ (45 640) was close to the theoretical one (46 420) of the dendrimer calculated from the absolute molecular weight of the building blocks (**5**, **10**, and **13**). The purity after preparative SEC increased to 97%. In addition, the ΔHDV calculated from the ratio of $M_{p,RI}$ to $M_{p,TD}$ was 0.72, which was close to the value used in the LND

Table 2. SEC, LND, and NMR Data for Dendrimers^a

dendrimer	reactants	$M_{n,RI}^b$	$M_{p,RI}^b$	PDI	$M_{n,TD}^c$	$M_{p,TD}^c$	PDI ^d	$M_{n,theo}^e$	ΔHDV		$M_{n,NMR}$	number of arms ^h			purity (%) ⁱ
									SEC ^f	LND ^g		G1	G2	G3	
14	5, 8, 12	26590	27650	1.08	35120	35990	1.05	33640	0.77	0.77	39340	4	8.20	8	94
15	5, 10, 12	29140	30520	1.07	37540	38590	1.05	38530	0.79	0.76	43990	4	8.12	16	96
16	5, 10, 13	31200	33360	1.08	45640	46330	1.03	46420	0.72	0.70	53540	4	8.14	16 ^j	97

^aAll the dendrimer products fractionated (purified) using preparative SEC. ^bMWD from SEC (RI). ^cMWD determined by DMAc triple detection SEC. ^dUnderestimation of true PDI value as light scattering has less sensitivity to low molecular weights. ^e $M_{n,theo}$ calculated from M_n of starting materials (Table 1). ^fHydrodynamic volume change (ΔHDV) determined from peak molecular weight ($\Delta HDV = M_{p,RI}/M_{p,TD}$). ^g ΔHDV used in log-normal distributions(LND) simulation. ^hDetermined from integration of each generation by ¹H NMR. ⁱDetermined from log-normal distributions(LND) simulation. ^jRepresents 16 units of dendron 13, which includes 16 and 32 L-lysine groups in the third- and fourth-generation layers, respectively.

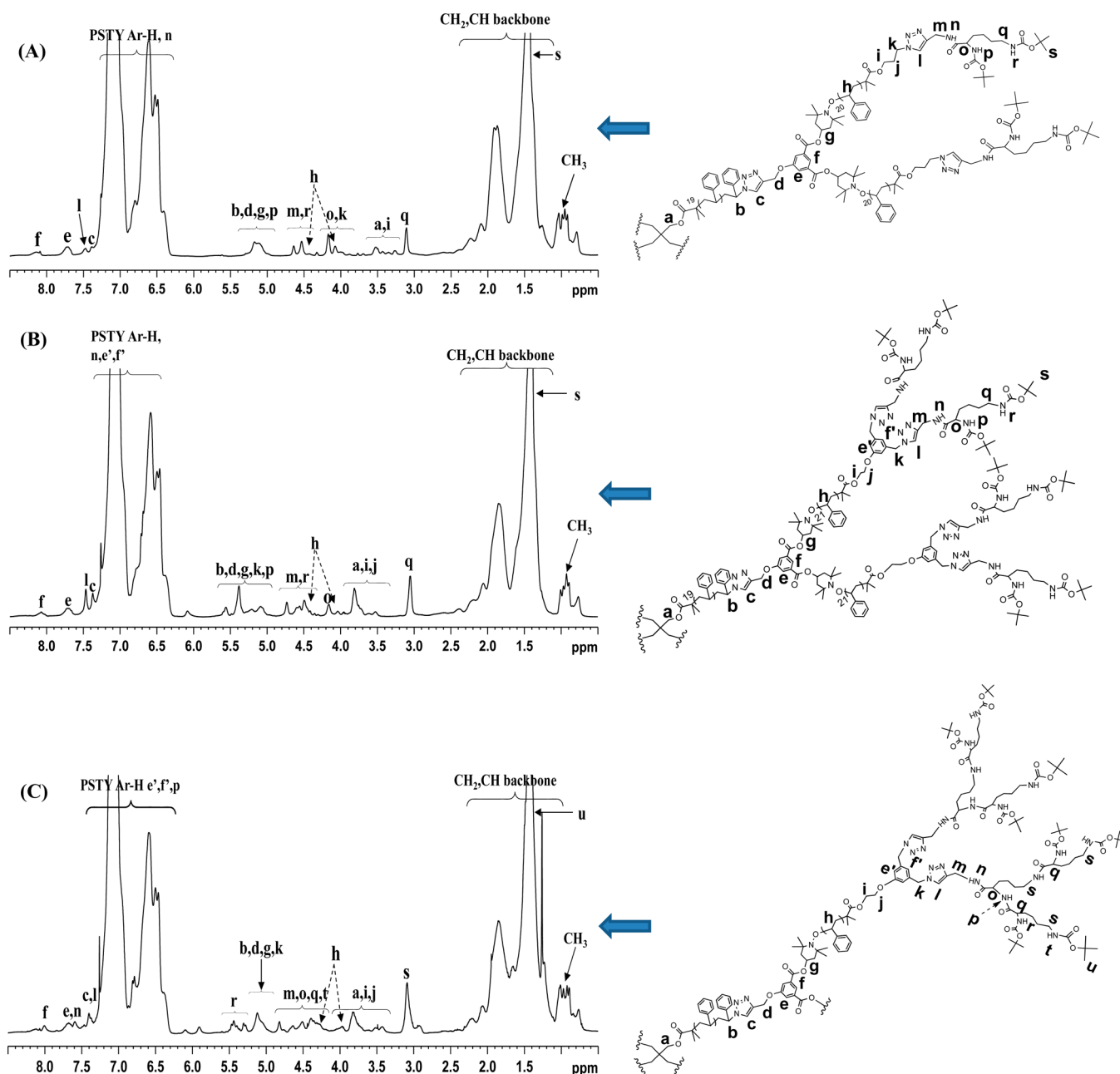


Figure 6. ¹H 1D DOSY NMR spectra of dendrimers (A) 14, (B) 15, and (C) 16, recorded in CDCl₃ at 298 K, 500 MHz; gradient strength (gpz6) 90%, gradient pulse length (p30) 2.5 ms.

simulation (Table 2). This lower ΔHDV value suggested that 16 was more compact due to the higher peripheral lysine

branching compared to either 14 or 15. Analysis by ¹H NMR further showed that the ratio of the number of arms in each

Table 3. Self-Assembly of Dendrimers in Water and Organic Solvents^a

dendrimer	THF		CDCl ₃			water			
	$D_{h,SEC}$ ^b (nm)	diffusion coefficient (m ² s ⁻¹) ^c	$D_{h,NMR}$ (nm) ^d	$D_{h,DLS}$ (nm)	PDI _{DLS}	$D_{h,TEM}$ (nm) ^e	$D_{h,DLS}$ (nm)	PDI _{DLS}	zeta potential (mV)
14	8.41	1.38×10^{-10}	5.97	5.80	0.168				
15	8.86	1.03×10^{-10}	8.00	8.44	0.164				
16	9.21	9.06×10^{-11}	9.06	10.44	0.228				
17						10.8	8.38	0.374	27.5
18						13.0	9.83	0.447	34.1
19						13.5	11.07	0.673	40.4

^aThe diameters were measured from three methods: (i) SEC, (ii) DOSY NMR, and (iii) DLS. ^bDetermined from eq 6 using the Mark–Houwink parameters ($K = 0.0141 \text{ cm}^3 \text{ g}^{-1}$, $a = 0.7$ in a good solvent). ^cDiffusion coefficient (D) determined by 2D DOSY NMR in CDCl₃ at 298 K. ^dDetermined from eq 2. ^eDetermined by averaging the size of over 50 particles in the TEM micrograph.

generational layer (i.e., 4:8.1:16:32) was close to theory (Figure 6C and Figure S25). The results taken together strongly support that all three polymeric dendrimers were produced in excellent purity. We could not obtain MALDI-ToF of the dendrimers, presumably due to the high molecular weights of the dendrimers.

Self-Assembly of Dendrimers in Organic and Aqueous Media. We used three different methods to determine the hydrodynamic diameter (D_h) in organic solvents. The first method used SEC to determine D_h in THF based on polystyrene standards.^{46,52} Using the Mark–Houwink relationship between molecular weight and intrinsic viscosity, one can determine the hydrodynamic radius (R_h) from the relationship⁵²

$$R_h^3 = \frac{3KM^{a+1}}{10\pi N_A} \quad (6)$$

where $K = 0.0141 \text{ cm}^3 \text{ g}^{-1}$, $a = 0.7$ (in a good solvent), and N_A is Avogadro's number. It can be seen from Table 3 that the $D_{h,SEC}$ increased from 8.41 to 9.21 nm for dendrimers 14 to 16 with an increase in the number of L-lysines on the periphery. It should be noted that the value of K is based on linear PSTY chains and would be expected to change for dendritic structures. The second and more precise method allowed determination of the diffusion coefficient (D) from a concentration-dependent diffusion-ordered NMR spectroscopy (DOSY).⁴⁴ The value of $D_{h,NMR}$ can be calculated from the Stokes–Einstein equation (see eq 2). The diameter (i.e., $D_{h,NMR}$) in CDCl₃ increased from 5.97 to 9.06 nm respectively for 14 to 16, which was supported from the very close values found by DLS (the third method). These sizes are expected, since the solvent is good for both PSTY and Boc-protected L-lysine to represent the unimolecular diameter (i.e., without aggregation or self-assembly of the dendrimers). In addition, the excellent agreement between the $D_{h,DLS}$ and $D_{h,NMR}$ suggests that the size determined by DLS is accurate and should provide some insight into the self-assembly of these dendrimers in water.

The self-assembly of L-lysine-decorated dendrimers into peptidomimetic nanoparticles represents the next step toward biological efficacy. The three Boc-protected L-lysine dendrimers were deprotected to the free L-lysine periphery by addition of TFA (Scheme 1). Micelles of three L-lysine dendrimers (17–19) were formed through the slow addition of water to a solution of dendrimer dissolved in DMF over a 6.5 h period and then further dialyzed with Milli-Q water for 2 days to remove organic solvent. It should be noted that there was a small amount of precipitant found after the self-assembly of 17.

All samples were filtered before analysis. The $D_{h,DLS}$ found in water increased from 8.38 to 11.07 nm for the three dendrimers 17 to 19 (Table 3). A similar trend was found from TEM (see Figure S32 in Supporting Information), although the TEM diameters ($D_{h,TEM}$) were slightly larger by ~ 2.5 nm. The zeta potential increased from +27.5 to +40.4 mV, as expected, with the increased number of cationic L-lysine groups on the periphery. The small size of the dendrimer micelles in water could be assumed to represent crew-cut unimolecular micelles or micelles with quite a low aggregation number. This postulate is in agreement with the low aggregation number found from the self-assembly of amphiphilic 4-arm block stars (consisting of an anionic outer block and a hydrophobic core block)^{53,54} and, more particularly, with the low aggregation number (Z) of 9 found for polymeric dendrimers decorated with anionic blocks.¹⁸ The reason for such low aggregation numbers compared to linear diblock copolymers (where Z ranges from 150 to 300)⁵³ is ascribed to junction points⁵⁵ and loops.⁵⁴ The PSTY core of our dendrimers consists of a 4-arm star tethered to a second-generational layer of linear PSTY with a cationic peripheral layer (i.e., L-lysine groups). The many junction points between PSTY building blocks results in stretching of the PSTY chains⁵¹ in the core, which further stretches due to the cationic peripheral groups. This stretching together with the formation of loops leads to an increase in the free energy, which can only be reduced by significantly lowering the aggregation number. Therefore, the data for our dendrimers suggests that the aggregation number is very low and consisting of unimolecular micelles (i.e., where $Z = 1$) and that the L-lysine groups on one side of the dendrimer must be as far from the L-lysine groups on the other side of the dendrimer to reduce loop formation and thus entropy, thus limiting the diameter to the length of a single dendrimer in the core. The dendrimer architecture also directed self-assembly toward spherical micelles compared to the lamella structure normally found from crew-cut diblock copolymer self-assembly.

CONCLUSION

In summary, we have demonstrated that by using copper to catalyze two orthogonal reactions (i.e., NRC and CuAAC) polymeric dendrimers with 3 and 4 generational layers could be constructed rapidly and with high purity. The purity of the 4-arm star core, 5, was essential to the success of creating polymeric dendrimers coated with L-lysine on the periphery. The ATRP of the 4-arm star produced 2, the precursor to 5, with a purity of 87.3% with the other 16.7% corresponding to higher molecular weight star–star coupling products. After purification by preparative SEC, the purity increased to 96.1%. Coupling various building blocks to 5, in a process where the

rates of reaction for the NRC and the CuAAC were similar (i.e., the parallel process), allowed us to produce three polymeric dendrimers with an increase in L-lysine peripheral density. The purity for **14**, **15**, and **16** was found to be 94, 96, and 97%, respectively, as determined using the LND method. Our work showed that the copper-catalyzed CuAAC and NRC reactions represent a powerful synthetic method to produce dendrimers in one pot at 25 °C. The versatility of this synthetic approach will have utility in the synthesis of polymeric dendrimers coated with a wide range of biomolecules. The self-assembly of these dendrimers in water demonstrates that due to the junction points within the dendrimer, the particle sizes were slightly larger than that found in organic solvents. We show here that utilizing amphiphilic dendrimers leads to control over the particles size due to its very low aggregation numbers. This represents an important step to implementing these peptidomimetic nanoparticles to increase the biological efficacy. We will carry out *in vitro* and *in vivo* studies in the future to confirm our hypothesis.

■ ASSOCIATED CONTENT

● Supporting Information

Synthesis and characterizations of all polymers, including ¹H NMR spectra, SEC traces, and MALDI-ToF spectra. This material is available free of charge via the Internet at <http://pubs.acs.org>.

■ AUTHOR INFORMATION

Corresponding Author

*E-mail: m.monteiro@uq.edu.au (M.J.M.).

Notes

The authors declare no competing financial interest.

■ ACKNOWLEDGMENTS

M.J.M. acknowledges financial support from the ARC Discovery grant (DP140103497).

■ REFERENCES

- (1) Kaspar, A. A.; Reichert, J. M. *Drug Discovery Today* **2013**, *18* (17–18), 807–817.
- (2) Vlieghe, P.; Lisowski, V.; Martinez, J.; Khrestchatsky, M. *Drug Discovery Today* **2010**, *15* (1–2), 40–56.
- (3) Bracci, L.; Falciani, C.; Lelli, B.; Lozzi, L.; Runci, Y.; Pini, A.; De Montis, M. G.; Tagliamonte, A.; Neri, P. *J. Biol. Chem.* **2003**, *278* (47), 46590–46595.
- (4) Jiang, Y. H.; Emau, P.; Cairns, J. S.; Flanary, L.; Morton, W. R.; McCarthy, T. D.; Tsai, C. C. *Aids Res. Hum. Retroviruses* **2005**, *21* (3), 207–213.
- (5) Bourne, N.; Stanberry, L. R.; Kern, E. R.; Holan, G.; Matthews, B.; Bernstein, D. I. *Antimicrob. Agents Chemother.* **2000**, *44* (9), 2471–2474.
- (6) Lee, C. C.; MacKay, J. A.; Frechet, J. M. J.; Szoka, F. C. *Nat. Biotechnol.* **2005**, *23* (12), 1517–1526.
- (7) Gajbhiye, V.; Palanirajan, V. K.; Tekade, R. K.; Jain, N. K. *J. Pharm. Pharmacol.* **2009**, *61* (8), 989–1003.
- (8) Percec, V.; Barboiu, B.; Grigoras, C.; Bera, T. K. *J. Am. Chem. Soc.* **2003**, *125* (21), 6503–6516.
- (9) Trollsas, M.; Hedrick, J. L. *J. Am. Chem. Soc.* **1998**, *120* (19), 4644–4651.
- (10) Hedrick, J. L.; Trollsas, M.; Hawker, C. J.; Atthoff, B.; Claesson, H.; Heise, A.; Miller, R. D.; Mecerreyes, D.; Jerome, R.; Dubois, P. *Macromolecules* **1998**, *31* (25), 8691–8705.
- (11) Matsuo, A.; Watanabe, T.; Hirao, A. *Macromolecules* **2004**, *37* (17), 6283–6290.
- (12) Whittaker, M. R.; Urbani, C. N.; Monteiro, M. J. *J. Am. Chem. Soc.* **2006**, *128* (35), 11360–11361.
- (13) Urbani, C. N.; Bell, C. A.; Lonsdale, D.; Whittaker, M. R.; Monteiro, M. J. *Macromolecules* **2008**, *41* (1), 76–86.
- (14) Urbani, C. N.; Bell, C. A.; Whittaker, M. R.; Monteiro, M. J. *Macromolecules* **2008**, *41* (4), 1057–1060.
- (15) Hossain, M. D.; Jia, Z. F.; Monteiro, M. J. *Macromolecules* **2014**, *47* (15), 4955–4970.
- (16) Skwarczynski, M.; Zaman, M.; Urbani, C. N.; Lin, I. C.; Jia, Z. F.; Batzloff, M. R.; Good, M. F.; Monteiro, M. F.; Toth, I. *Angew. Chem., Int. Ed.* **2010**, *49* (33), 5742–5745.
- (17) Liu, T. Y.; Hussein, W. M.; Jia, Z. F.; Ziora, Z. M.; McMillan, N. A. J.; Monteiro, M. J.; Toth, I.; Skwarczynski, M. *Biomacromolecules* **2013**, *14* (8), 2798–2806.
- (18) Lonsdale, D. E.; Whittaker, M. R.; Monteiro, M. J. *J. Polym. Sci., Part A: Polym. Chem.* **2009**, *47* (22), 6292–6303.
- (19) Bell, C. A.; Jia, Z. F.; Kulis, J.; Monteiro, M. J. *Macromolecules* **2011**, *44* (12), 4814–4827.
- (20) Trollsas, M.; Claesson, H.; Atthoff, B.; Hedrick, J. L. *Angew. Chem., Int. Ed.* **1998**, *37* (22), 3132–3136.
- (21) Trollsas, M.; Atthof, B.; Wursch, A.; Hedrick, J. L.; Pople, J. A.; Gast, A. P. *Macromolecules* **2000**, *33* (17), 6423–6438.
- (22) Lammens, M.; Fournier, D.; Fijten, M. W. M.; Hoogenboom, R.; Du Prez, F. *Macromol. Rapid Commun.* **2009**, *30* (23), 2049–2055.
- (23) Urbani, C. N.; Lonsdale, D. E.; Bell, C. A.; Whittaker, M. R.; Monteiro, M. J. *J. Polym. Sci., Part A: Polym. Chem.* **2008**, *46* (5), 1533–1547.
- (24) Urbani, C. N.; Bell, C. A.; Lonsdale, D. E.; Whittaker, M. R.; Monteiro, M. J. *Macromolecules* **2007**, *40* (19), 7056–7059.
- (25) Hutchings, L. R.; Roberts-Bleming, S. J. *Macromolecules* **2006**, *39* (6), 2144–2152.
- (26) Konkolewicz, D.; Monteiro, M. J.; Petrie, S. *Macromolecules* **2011**, *44* (18), 7067–7087.
- (27) Kimani, S. M.; Hutchings, L. R. *Macromol. Rapid Commun.* **2008**, *29* (8), 633–637.
- (28) Hutchings, L. R. *Soft Matter* **2008**, *4* (11), 2150–2159.
- (29) Hu, D.; Zheng, S. X. *Eur. Polym. J.* **2009**, *45* (12), 3326–3338.
- (30) Pan, P. J.; Fujita, M.; Ooi, W. Y.; Sudesh, K.; Takarada, T.; Goto, A.; Maeda, M. *Polymer* **2011**, *52* (4), 895–900.
- (31) Lutz, J. F.; Borner, H. G.; Weichenhan, K. *Macromolecules* **2006**, *39* (19), 6376–6383.
- (32) Sumerlin, B. S.; Vogt, A. P. *Macromolecules* **2010**, *43* (1), 1–13.
- (33) Inglis, A. J.; Sinnwell, S.; Stenzel, M. H.; Barner-Kowollik, C. *Angew. Chem., Int. Ed.* **2009**, *48* (13), 2411–2414.
- (34) Kade, M. J.; Burke, D. J.; Hawker, C. J. *J. Polym. Sci., Part A: Polym. Chem.* **2010**, *48* (4), 743–750.
- (35) Campos, L. M.; Killups, K. L.; Sakai, R.; Paulusse, J. M. J.; Damiron, D.; Drockenmuller, E.; Messmore, B. W.; Hawker, C. J. *Macromolecules* **2008**, *41* (19), 7063–7070.
- (36) Campos, L. M.; Meinel, I.; Guino, R. G.; Schierhorn, M.; Gupta, N.; Stucky, G. D.; Hawker, C. J. *Adv. Mater.* **2008**, *20* (19), 3728–+.
- (37) Killups, K. L.; Campos, L. M.; Hawker, C. J. *J. Am. Chem. Soc.* **2008**, *130* (15), 5062–+.
- (38) Antoni, P.; Robb, M. J.; Campos, L.; Montanez, M.; Hult, A.; Malmstrom, E.; Malkoch, M.; Hawker, C. J. *Macromolecules* **2010**, *43* (16), 6625–6631.
- (39) Ma, X. P.; Tang, J. B.; Shen, Y. Q.; Fan, M. H.; Tang, H. D.; Radosz, M. *J. Am. Chem. Soc.* **2009**, *131* (41), 14795–14803.
- (40) Jia, Z. F.; Bell, C. A.; Monteiro, M. J. *Chem. Commun.* **2011**, *47* (14), 4165–4167.
- (41) Matyjaszewski, K.; Davis, T. P. *Handbook of Radical Polymerization*; John Wiley and Sons: New York, 2002.
- (42) Mantovani, G.; Ladmiral, V.; Tao, L.; Haddleton, D. M. *Chem. Commun.* **2005**, No. 16, 2089–2091.
- (43) Agrawal, P.; Gupta, U.; Jain, N. K. *Biomaterials* **2007**, *28* (22), 3349–3359.
- (44) Altintas, O.; Krolla-Sidenstein, P.; Gliemann, H.; Barner-Kowollik, C. *Macromolecules* **2014**, *47* (17), 5877–5888.

- (45) Gavrilov, M.; Monteiro, M. J. *Eur. Polym. J.* **2015**, DOI: 10.1016/j.eurpolymj.2014.11.018.
- (46) Monteiro, M. J. *Eur. Polym. J.* **2015**, DOI: 10.1016/j.eurpolymj.2015.01.009.
- (47) Kulis, J.; Bell, C. A.; Micallef, A. S.; Jia, Z. F.; Monteiro, M. J. *Macromolecules* **2009**, *42* (21), 8218–8227.
- (48) Kulis, J.; Bell, C. A.; Micallef, A. S.; Monteiro, M. J. *J. Polym. Sci., Part A: Polym. Chem.* **2010**, *48* (10), 2214–2223.
- (49) Percec, V.; Guliashvili, T.; Ladislaw, J. S.; Wistrand, A.; Stjern Dahl, A.; Sienkowska, M. J.; Monteiro, M. J.; Sahoo, S. *J. Am. Chem. Soc.* **2006**, *128* (43), 14156–14165.
- (50) Kulis, J.; Jia, Z. F.; Monteiro, M. J. *Macromolecules* **2012**, *45* (15), 5956–5966.
- (51) Daoud, M.; Cotton, J. P. *J. Phys. (Paris)* **1982**, *43* (3), 531–538.
- (52) Hossain, M. D.; Lu, D. R.; Jia, Z. F.; Monteiro, M. J. *ACS Macro Lett.* **2014**, *3* (12), 1254–1257.
- (53) Whittaker, M. R.; Monteiro, M. J. *Langmuir* **2006**, *22* (23), 9746–9752.
- (54) Iatrou, H.; Willner, L.; Hadjichristidis, N.; Halperin, A.; Richter, D. *Macromolecules* **1996**, *29* (2), 581–591.
- (55) Kim, K. H.; Kim, S. H.; Huh, J.; Jo, W. H. *J. Chem. Phys.* **2003**, *119* (11), 5705–5710.